Tribol Lett (2013) 51:1–7
DOI 10.1007/s11249-013-0156-4

METHODS PAPER

Identifying Erosion Mechanism: A Novel Approach

H. S. Grewal · Anupam Agrawal · H. Singh

Received: 3 January 2013 / Accepted: 7 May 2013 / Published online: 17 May 2013

Abstract Understanding the erosion mechanism is a key to improve the performance of material subjected to erosive condition. Capability to predict the erosion mechanism could prove to be useful tool. In this work, a parameter named "erosion mechanism identifier," ξ, is proposed to predict the erosion mechanism in materials. Suitability of ξ in predicting erosion mechanism of ductile and brittle materials was evaluated using the data reported in the literature. It was observed that ξ is able to predict the erosion mechanism for both categories of material. The predictability of ξ was not restrained by different operating conditions.

Keywords Erosive wear · Wear mechanisms · Tribology databases · Hardness

List of symbols

E Erosion rate
H Hardness
K Toughness
V Volume loss
m Mass of erodent particles
v Velocity of erodent particles

Greek symbols

η Erosion efficiency
ξ Erosion mechanism identifier
σ Critical stress
σ_u Ultimate tensile strength
σ_R Transverse rupture strength
τ_u Ultimate shear strength

H. S. Grewal · A. Agrawal · H. Singh (✉)
School of Mechanical, Materials and Energy Engineering, Indian Institute of Technology Ropar, Nangal Road, Rupnagar 140001, Punjab, India
e-mail: harpreetsingh@iitrpr.ac.in; hn1998@gmail.com

1 Introduction

Erosion is a type of wear wherein the degradation of the solid target surface takes places due to impingement of solid and/or liquid particles. Slurry erosion is a type of erosion wherein material is removed from the target surface due to impingement of solid particles entrained in liquid medium. It is termed as solid particle erosion if in place of liquid, air acts as a carrier medium. The mechanism responsible for removal of material is the function of operating parameters, among which velocity (v) and angle of impingement (θ) are most influential.

Understanding erosion mechanism is very important as it can help in identifying prominent properties that control the erosion performance. With this knowledge, one can improve the performance of erosion effected systems by employing more suitable structural materials. Identification of erosion mechanism is usually undertaken by studying the dependence of erosion behavior upon angle of impingement. Material that shows highest erosion rate at low angles (15°–30°) is said to exhibit ductile mode of erosion [1–5]. On the other hand, if maximum erosion rate is observed at 90° angle, material loss is said to have taken place through brittle erosion mode [1–5]. However, as also pointed out by Sundararajan [6], this kind of crude distinction of erosion mechanism based on dependence of erosion behavior on θ is not appropriate. Depending upon the shape and hardness of erodent particles, the dependence of erosion behavior on θ can be totally altered. Ductile materials can show higher erosion rates at 90° angle, whereas brittle materials can exhibit maximum erosion at low impingement angles [2, 7–11].

2 Theory

Zum Gahr [12] proposed a model for abrasive wear which could help in identifying the material removal mechanism. For erosion, Sundararajan [6] proposed a parameter "erosion efficiency," η, which could help in predicting the erosion mechanism in different materials. However, after Sundararajan [6], no further work in this direction was pursued. In his model given in Eq. (1), Sundararajan [6] considered η as the ratio of the volume of material removed to the volume of crater formed. The volume of the crater formed was assumed to be the function of hardness of the target material. In Eq. (1), H is hardness of the target material, V_r, the volume of material removed, m and v, the mass and velocity of the erodent particles, respectively. This model was developed with an assumption that erodent particles impact the solid surface at 90° angle. The value of dimensionless η was related to the erosion mechanism. If $\eta > 1$; then, brittle mechanism is said to occur, however, if $\eta < 1$, plastic deformations are assumed to control the erosion mechanism. On the other hand, if η is equal to 1, microcutting is said to persist. The authors have used the data for erosion rates from the literature [13–22] so as to test the validity of η under wide range of parameters and materials.

$$\eta = \frac{\mathrm{HV}}{0.5\ \mathrm{mv}^2} \tag{1}$$

From the results discussed in next section, it can be observed that η fails to predict accurately the erosion mechanism for cast irons. Along with this, the inability of η to predict erosion mechanism at angles <90° has motivated the authors to devise new model, which could overcome these issues.

To improve the predictability of the erosion mechanism, a new parameter "erosion mechanism identifier," ξ, is proposed in present work. ξ is considered to be the ratio of specific energies as shown in Eq. (2). Here, SER is the specific energy required for the removal of the unit volume of material, whereas SEE is the specific energy expended in removing unit volume of material.

$$\xi = \frac{\mathrm{SER}}{\mathrm{SEE}} \tag{2}$$

SER is further considered to be the function of hardness (H), toughness (K), and critical stress (σ) of the target material, Eq. (3). Critical stress (σ) depends upon the type of material. For brittle metals and alloys, σ is considered to be

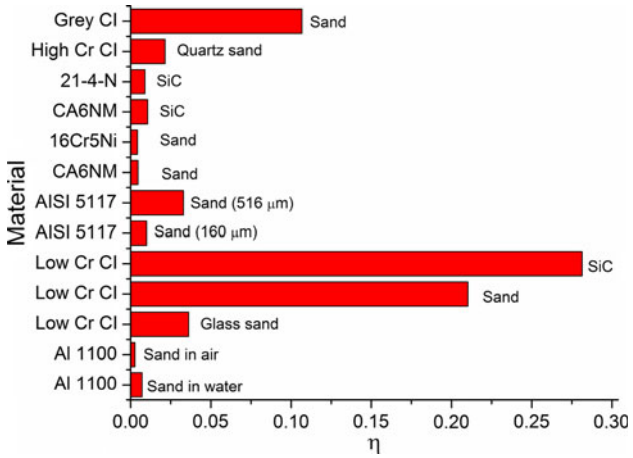

Fig. 1 Values of "erosion efficiency," η for various materials eroded at 90° impingement angle under different operating conditions indicated against each case

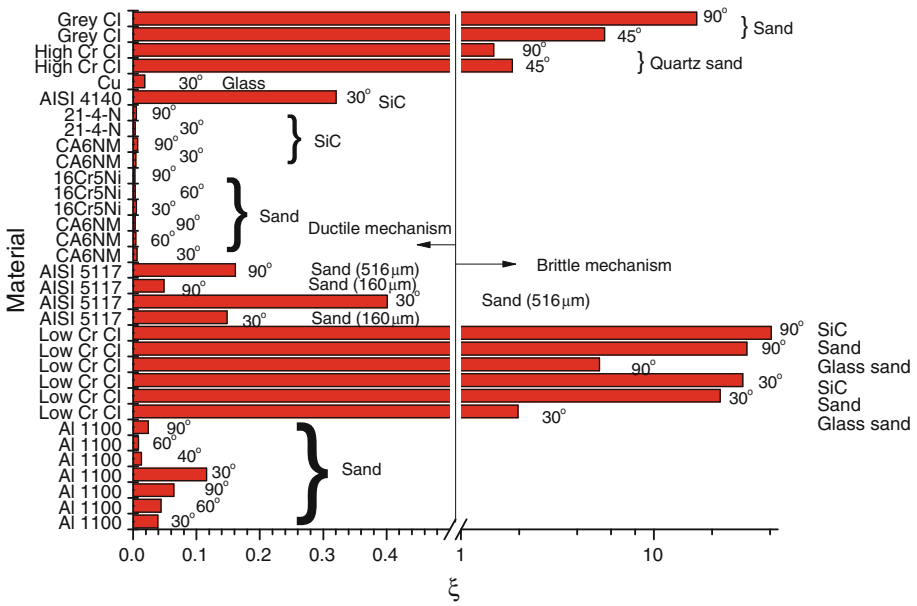

Fig. 2 Value of "erosion mechanism identifier," ξ, for different metals and alloys eroded at different operating conditions indicated along each case

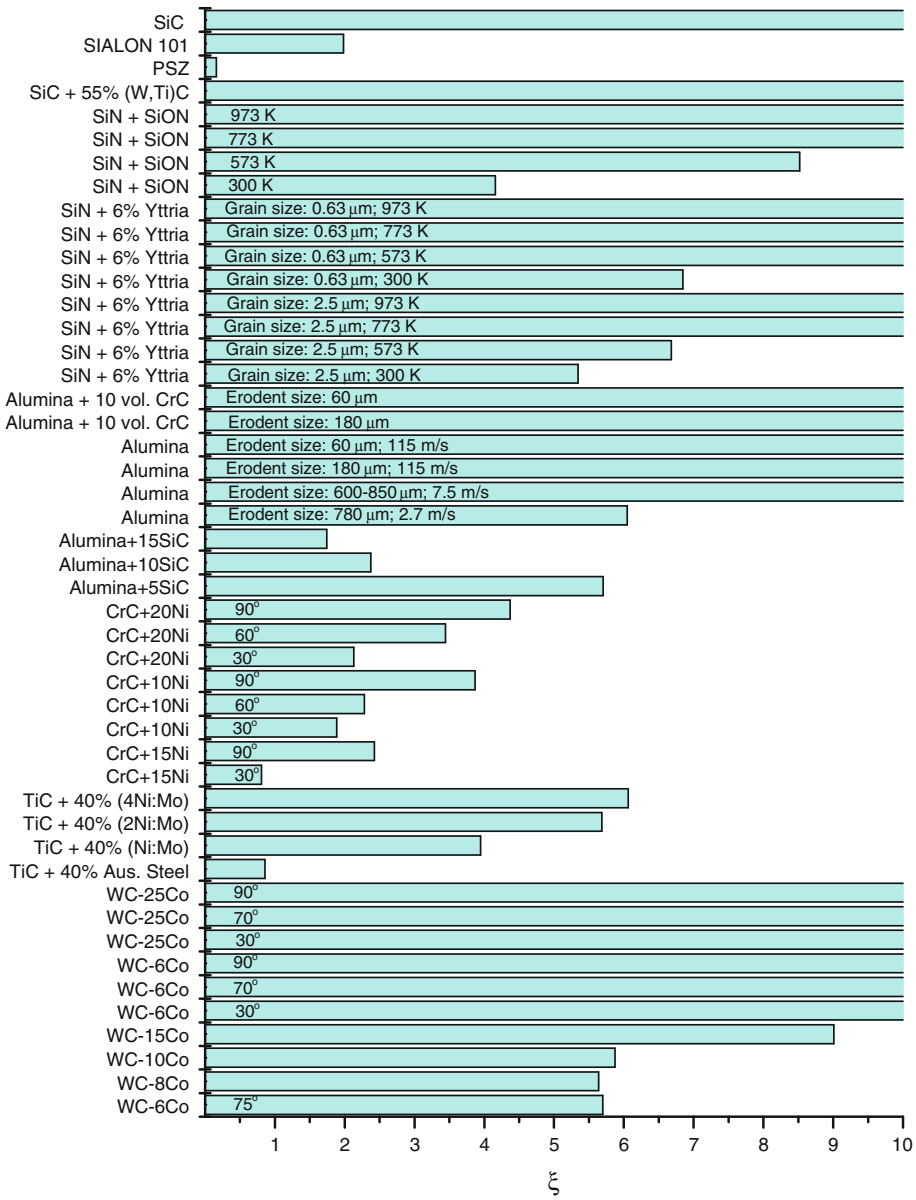

Fig. 3 Value of "erosion mechanism identifier," ξ, for different class of materials (ceramics, cermets, and composites) with different operating conditions indicated for similar materials. Here, CrC–Cr_3C_2, SiN–Si_3N_4, SiON–Si_2ON_2, PSZ—partially stabilized zirconia

equal to ultimate tensile strength (σ_u) whereas, in case of cermets, ceramics, and composites, transverse rupture strength (σ_R) was considered. For ductile materials, σ is taken equivalent to ultimate shear stress (τ_u). These are usually the limiting stresses responsible for failure of materials. Being the function of H, K, and σ, the expression for SER is proposed as given in Eq. (4). The ratio of H and K in Eq. (4) represents the brittleness of the material [23]. Although different forms of this function are equally possible, however, convergence to the present form was based upon the fact that the final expression should be dimensionless. Additionally, brittleness has direct correlation with the erosion performance of the material [23–25]. With these at the backend, the function for SER reduced to the form shown in Eq. (4). Within same category of material, it has also been observed that with rise in hardness, the erosion rate reduces.

$$\mathrm{SER} = f(H, K, \sigma) \tag{3}$$

$$\mathrm{SER} = \left(\frac{H}{K}\right) \times \sigma \tag{4}$$

Now, SEE, the amount of energy expanded for removing unit volume of material is given by Eq. (5). Here, m is the total mass of the erodents used in erosion testing and v is the average velocity of these erodent particles coming out of the nozzle. V is the volume of the material removed due to impingement of erodents of mass, m. Substituting the expressions for SER and SEE from Eqs. (4) and (5), respectively, in Eq. (2), the expression for

erosion mechanism identifier, ξ, is shown in Eq. (6). Alternatively, Eq. (7) can be used; in case erosion rate, E (m^3/Kg) is available.

$$\mathrm{SEE} = \frac{0.5\ mv^2}{V} \tag{5}$$

$$\xi = \frac{V\sigma\left(\frac{H}{K}\right)}{0.5\ mv^2} \tag{6}$$

$$\xi = \frac{E\sigma\left(\frac{H}{K}\right)}{0.5\ v^2} \tag{7}$$

Erosion mechanism identifier, ξ, being the ratio of the specific energies is a dimensionless term, and value of this ξ could be used for predicting the erosion mechanism. When SER is smaller than SEE, it would give $\xi < 1$. It means that we need to expend more energy than that required for the removal of unit volume of material. It is to be noticed that removal of material through plastic deformation is a slow process. It requires large number of impingement of erodents to remove material [26]. Both ploughing and platelet mechanism of erosion belongs to this category of erosion mechanism. On the other hand, when SER is greater than SEE, it means that we need to expend low amount of energy than required to remove unit volume of material. This condition would be met when removal of material takes place thought cracking and spalling, a brittle erosion mode. This would result in value of $\xi > 1$. When ξ is equal to 1, SER would be equal to SEE. It is to be considered that this condition would be met when energy expended would be just equivalent to that required for erosion. This balance is met in microcutting, where material is removed through shearing process.

3 Results and Discussion

The values of η for different categories of materials at $\theta = 90°$ are shown in Fig. 1. Along with each case, a remark could be found which either indicates the type of erodent particle or indicates the average particle size. It can be observed that η fails to predict accurately the erosion mechanism for cast irons. Three types of cast irons (gray, low Cr, and high Cr) were studied here; however, it can be observed that for all these cast irons, η is <1 (Fig. 1). This indicates the plastic deformations being the prominent erosion mechanism for cast irons, which otherwise is opposite to the actual observations. Cast irons normally erode in brittle manner through cracking and spalling.

The value of ξ for different categories of materials eroded under various operating conditions is shown in Figs. 2 and 3 using the results reported in the literature [9–38]. The values of H, K, and σ used for calculating ξ are given in Tables 1 and 2. It was observed that although a large amount of the literature is available in the field of mechanical erosion, however, most of it could not be used here due to lack of reported data. The required values of K and σ could not be found for majority of the cases, especially for ceramic and

Table 1 Mechanical properties of different metals and alloys used in calculating the values of "erosion efficiency," η and "erosion mechanism identifier," ξ

Material	Hardness, H (HV)	Toughness, K (Mpa)	Critical stress, σ (MPa)
Al 1100	38.5	10.0	89.7
Low Cr cast iron	778	7.0	1,011
AISI 5117 steel	200	115.8	568
CA6NM steel	336	1,025	697
16Cr5Ni steel	352	1,100	750
21Cr4N steel	320	900	507
AISI 4140 steel	190	42.0	461
Copper	39.6	17.0	100
High Cr cast iron	591	7.0	689
Gray cast iron	180	1.6	250

Table 2 Mechanical properties of different cermets, ceramics, and composites used for calculating the values of "erosion mechanism identifier," ξ

Material	Hardness, H (HV)	Fracture toughness, K (Mpa$\sqrt{m}$)	Critical stress, σ (MPa)
WC-6Co	1,315	8.5–16	2,210
WC-8Co	1,292	10.5	1,500
WC-10Co	1,224	12	1,595
WC-15Co	1,029	15.8	2,371
WC-25Co	950	25	2,500
TiC + 40 % FeCr7Si1.7	1,360	13.2	2,000
TiC + 40 % (Ni:Mo)	1,330	17.5	890
TiC + 40 % (2Ni:Mo)	1,200	17.8	1,320
TiC + 40 % (4Ni:Mo)	1,068	18.2	1,430
Cr_3C_2 + 15Ni	1,410	9.8	900
Cr_3C_2 + 10Ni	1,450	7.8	960
Cr_3C_2 + 20Ni	1,270	14.2	1,100
Al_2O_3	1,790–1,500	3.5–4.2	431–380
Al_2O_3 + 5SiC	1,930	5.1	646
Al_2O_3 + 10SiC	2,010	5.2	560
Al_2O_3 + 15SiC	2,080	5.4	549
Al_2O_3 + 10 vol. Cr_3C_2	1,680	5.1	495
Si_3N_4	1,450	6.5	945
Si_3N_4 + 6 % Y_2O_5	1,420–1,530	4.9–4.3	664–1,108
Si_3N_4 + Si_2N_2O	1,530	4.6	1,085
SIALON 101	1,675	3	945
Partially stabilized zirconia (PSZ)	1,489	6	700
SiC + 55 % (W,Ti)C	2,550	4.92	548.6
SiC	2,255	2.8	550

cermets. Therefore, in place of toughness, fracture toughness was used when investigating the ceramics, cermets, and composites. Further, transverse rupture strength was used as a critical stress for these classes of materials. In Table 1, wherever the values of K or σ were not reported by investigators were obtained from Ref [39]. Micrographs showing the erosion mechanisms of different class of materials could be found in Fig. 4.

From Fig. 2, it can be observed that ξ is more useful in predicting the erosion mechanism in comparison with η. It can be observed that value of ξ for cast irons is greater than 1, whereas for all other materials representing the ductile category of materials, ξ is less than 1. The erosion mechanism in three different grades of cast iron was effectively predicted by ξ. Moreover, ξ was also able to predict the erosion mechanism at different impingement angles, a

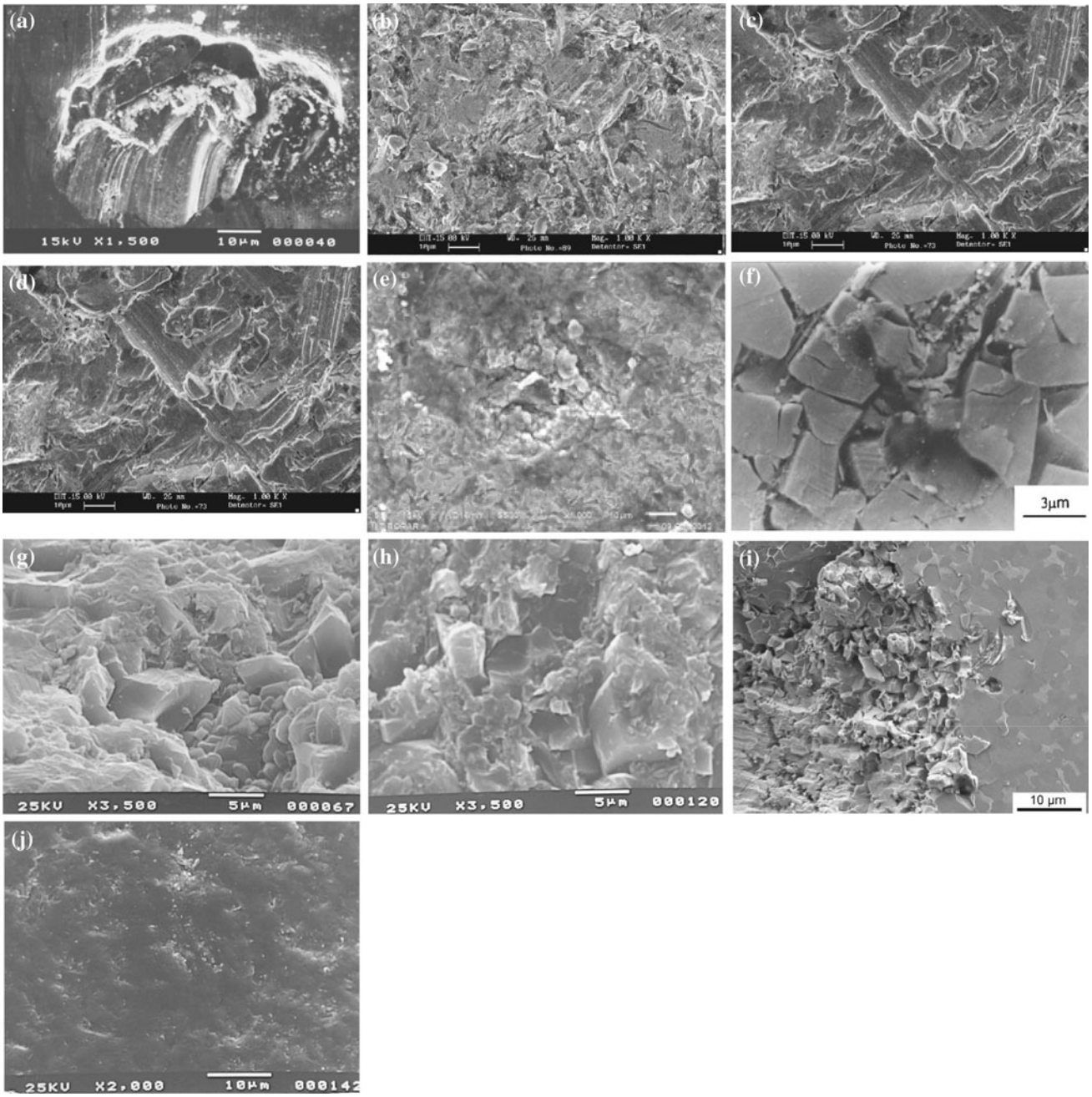

Fig. 4 SEM micrographs illustrating the morphology of the eroded surfaces of various materials at different operating conditions. **a** AISI 5117 steel eroded at 30° [15]. **b** 21-4-N steel eroded at 30° [17, 18]. **c** CA6NM steel eroded at 30° [17, 18]. **d** CA6NM steel eroded at 90° [17, 18]. **e** Cast iron eroded at 45° [22]. **f** WC–Co eroded at 75° [27]. **g** Alumina eroded at 90° [35]. **h** SiC eroded [35]. **i** Cr_3C_2 + 20 % Ni eroded at 60° [33]. **j** Zirconia (PSZ) [35]

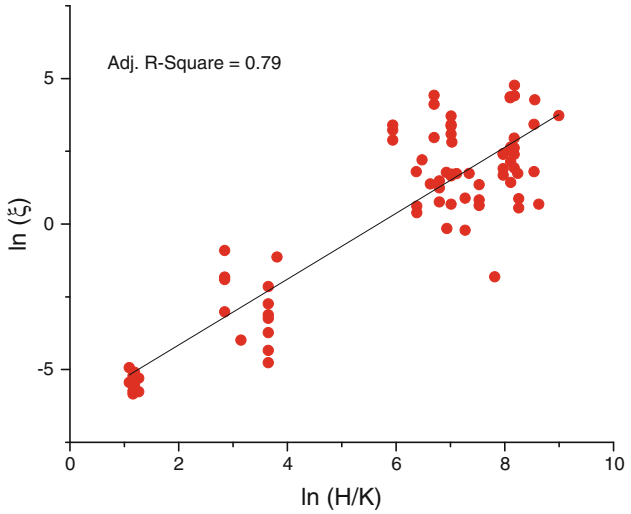

Fig. 5 Correlation between the brittleness and "erosion mechanism identifier," ξ

limitation observed in case of η. For $\theta = 45°$, gray cast iron showed a brittle mechanism [22] as also predicted by ξ. A scanning electron microscopic micrograph of the eroded surface of cast iron as shown in Fig. 4e confirms this prediction. Here, craters formed due to brittle fracture could be clearly observed. For comprehensiveness, morphology of eroded materials showing ductile mode of erosion has also been shown in Fig. 4a–d.

Figure 3 further highlights the predictive capabilities of the ξ. Here, erosion mechanism of other categories of materials viz. cermets, ceramics, and composites was predicted using ξ. It can be observed that ξ successfully predicts the erosion mechanism of these materials as well. With the exception of zirconia (PSZ), value of ξ for all other materials ≥ 1, this indicates the dominance of brittle erosion mode. In case of zirconia (PSZ), value of ξ was <1, represents the predominance of ductile erosion mechanism. Although zirconia belongs to the brittle class of materials, however, it still showed ductile erosion mode which could also be observed from Fig. 4j [35]. Fang et al. [35], while conducting investigations on zirconia, also suggested that it shows ductile erosion mechanism. This further strengthens the predictive capabilities of ξ.

The variation in ξ with brittleness (H/K) is shown in Fig. 5, which is a log–log plot. Although highly scattered, a linear correlation between ξ and brittleness could be expected. Correlation parameters, Adj. R^2 of around 0.79, were found while fitting a linear curve to these data point. Correlation dependence of this level do indicates some linear dependency between the ξ and brittleness (H/K). This indicates that brittleness plays a dominant role in controlling the erosion mechanism of the materials. With an increase in brittleness, the tendency of material to erode through brittle mode also increases. However, there must be some transition level, beyond which the erosion mechanism exhibited by the material transits from one mode to another. Therefore, it can be concluded that for improved erosion resistance, other than hardness and/or toughness, brittleness of the material should also be taken into account. A material with high brittleness could be expected to exhibit low resistance against erosion.

4 Conclusion

A new parameter named "erosion mechanism identifier" (ξ) was introduced in this work which could help in predicting the erosion mechanism in materials. In comparison with existing parameter (erosion efficiency), the proposed parameters were able to predict the erosion mechanism more accurately. This new parameter addressed the limitations of the older one and facilitated the erosion mechanism prediction at different operating conditions. A linear correlation between the brittleness and ξ was also observed. It indicates that the tendency of material to exhibit brittle erosion mechanism increases with increase in brittleness.

Acknowledgments Authors thankfully acknowledge the financial assistance provided by Council of Scientific and Industrial Research (CSIR), India, under project title "*Development of Slurry Erosion Resistant Coatings for Hydroturbines,*" File no.: 22(0604)/12/EMR-II.

References

1. Finnie, I.: Some reflections on the past and future of erosion. Wear **186–187**, 1–10 (1995)
2. Stachowiak, G.W., Batchelor, A.W.: Engineering Tribology. Butterworth-Heinemann, Burlington (2005)
3. Levy, A.V.: Solid Particle Erosion and Erosion-Corrosion of Materials. ASM International, Ohio (1995)
4. Finnie, I.: Erosion of surfaces by solid particles. Wear **3**(2), 87–103 (1960)
5. Hutchings, I.M.: Tribology: Friction and Wear of Engineering Materials. Edward Arnold, London (1992)
6. Sundararajan, G., Roy, M., Venkataraman, B.: Erosion efficiency-a new parameter to characterize the dominant erosion micromechanism. Wear **140**(2), 369–381 (1990)
7. Kleis, I.: Probleme der Bestimmung des Strahlverschleisses bei metallen. Wear **13**(3), 199–215 (1969)
8. Cousens, A.K., Hutchings, I.M.: A critical study of the erosion of an aluminium alloy by solid spherical particles at normal impingement. Wear **88**(3), 335–348 (1983)
9. Reddy, A.V., Sundararajan, G.: Erosion behaviour of ductile materials with a spherical non-friable erodent. Wear **111**(3), 313–323 (1986)
10. Sheldon, G.L., Finnie, I.: On the ductile behavior of nominally brittle materials during erosive cutting. J. Eng. Ind. **88**(4), 387–392 (1966)
11. IImar Kleis, P.K.: Solid Particle Erosion: Occurrence Prediction and Control. Springer, London (2008)
12. Gahr, K.H.Z.: Modelling of two-body abrasive wear. Wear **124**(1), 87–103 (1988)

13. Zu, J.B., Burstein, G.T., Hutchings, I.M.: A comparative study of the slurry erosion and free-fall particle erosion of aluminium. Wear **149**(1–2), 73–84 (1991)
14. Guo, D.Z., Wang, L.J., Li, J.Z.: Erosive wear of low chromium white cast iron. Wear **161**(1–2), 173–178 (1993)
15. Abouel-Kasem, A.: Particle size effects on slurry erosion of 5117 steels. J. Tribol. **133**(1), 014502 (2011)
16. Grewal, H.S., Bhandari, S., Singh, H.: Parametric study of slurry-erosion of hydroturbine steels with and without detonation gun spray coatings using taguchi technique. Metall. Mater. Trans. A **43**(9), 3387–3401 (2012)
17. Chauhan, A.K., Goel, D.B., Prakash, S.: Erosion behaviour of hydro turbine steels. Bull. Mater. Sci. **31**(2), 115–120 (2008)
18. Chauhan, A.K., Goel, D.B., Prakash, S.: Solid particle erosion behaviour of 13Cr–4Ni and 21Cr–4Ni–N steels. J. Alloy. Compd. **467**(1–2), 459–464 (2009)
19. Ambrosini, L., Bahadur, S.: Erosion of AISI 4140 steel. Wear **117**(1), 37–48 (1987)
20. Brown, R., Edington, J.W.: Erosion of copper single crystals under conditions of 30° incidence. Wear **79**(3), 335–346 (1982)
21. Fuyan, L., Hesheng, S.: The effect of impingement angle on slurry erosion. Wear **141**(2), 279–289 (1991)
22. Grewal, H.S., Singh, H.: To Study the Effect of Impingement Angle on Slurry Erosion Behaviour of Aluminium and Cast Iron. Report (2012)
23. Wright, I.G., Shetty, D.K., Clauer, A.H.: Slurry erosion of WC-Co cermets and its relationship to materials properties. In: Field, J.E., Corney, N.S. (eds.) Proceedings 6th International Conference Erosion by Liquid and Solid Impact, Cambridge, UK September 1983. Cavendish Laboratory, University of Cambridge, Cambridge (1983)
24. Fang, Q., Sidky, P.S., Hocking, M.G.: Erosion and corrosion of PSZ-zirconia and the t-m phase transformation. Wear **233–235**, 615–622 (1999)
25. Oka, Y.I., Yoshida, T.: Practical estimation of erosion damage caused by solid particle impact: part 2: mechanical properties of materials directly associated with erosion damage. Wear **259**(1–6), 102–109 (2005)
26. Bellman Jr, R., Levy, A.: Erosion mechanism in ductile metals. Wear **70**(1), 1–27 (1981)
27. Allen, C., Sheen, M., Williams, J., Pugsley, V.A.: The wear of ultrafine WC-Co hard metals. Wear **250**(1–12), 604–610 (2001)
28. Beste, U., Hammerström, L., Engqvist, H., Rimlinger, S., Jacobson, S.: Particle erosion of cemented carbides with low Co content. Wear **250**(1–12), 809–817 (2001)
29. Bhagat, R.B., Conway Jr, J.C., Amateau, M.F., Brezler Iii, R.A.: Tribological performance evaluation of tungsten carbide-based cermets and development of a fracture mechanics wear model. Wear **201**(1–2), 233–243 (1996)
30. Hussainova, I., Kolesnikova, A., Hussainov, M., Romanov, A.: Effect of thermo-elastic residual stresses on erosive performance of cermets with core-rim structured ceramic grains. Wear **267**(1–4), 177–185 (2009)
31. Hussainova, I., Kubarsepp, J., Pirso, J.: Mechanical properties and features of erosion of cermets. Wear **250**(1–12), 818–825 (2001)
32. Hussainova, I.: Microstructure and erosive wear in ceramic-based composites. Wear **258**(1–4), 357–365 (2005)
33. Hussainova, I., Pirso, J., Antonov, M., Juhani, K., Letunovits, S.: Erosion and abrasion of chromium carbide based cermets produced by different methods. Wear **263**(7–12), 905–911 (2007)
34. Anya, C.C.: Wet erosive wear of alumina and its composites with SiC nano-particles. Ceram. Int. **24**(7), 533–542 (1998)
35. Fang, Q., Xu, H., Sidky, P.S., Hocking, M.G.: Erosion of ceramic materials by a sand/water slurry jet. Wear **224**(2), 183–193 (1999)
36. Jeng, C.-A., Huang, J.-L., Lee, S.-Y., Hwang, B.-H.: Erosion damage and surface residual stress of Cr3C2/Al2O3 composite. Mater. Chem. Phys. **78**(1), 278–287 (2003)
37. Choi, H.-J., Han, D.-H., Park, D.-S., Kim, H.-D., Han, B.-D., Lim, D.-S., Kim, I.-S.: Erosion characteristics of silicon nitride ceramics. Ceram. Int. **29**(6), 713–719 (2003)
38. Deng, J.: Wear behaviors of ceramic nozzles with laminated structure at their entry. Wear **266**(1–2), 30–36 (2009)
39. ASM International: Atlas of Stress-Strain Curves. ASM International, Materials Park, OH (2002)